Research in Astron. Astrophys. **2009** Vol. **9** No. **8**, 883 – 887
*http://www.raa-journal.org* *http://www.iop.org/journals/raa*

*Research in Astronomy and Astrophysics*

# Measurements of the equivalent thicknesses of three-dimensional spiral galactic disks *

Gang Li[1], Zhi-Quan Luo[1] and Qiu-He Peng[2]

[1] Institute of Theoretical Physics, China West Normal University, Nanchong 637002, China; *zqluo@tom.com*

[2] Department of Astronomy, Nanjing University, Nanjing 210093, China

Received 2009 January 9; accepted 2009 March 22

**Abstract** Spiral arms are fitted after the data from the latest spiral galactic images released by the Sloan Digital Sky Survey are processed. Equivalent thicknesses of 42 spiral galactic disks are derived, which increase the foundational data for further research about spiral galaxies.

**Key words:** galaxies: spiral — Galaxy: disk

## 1 INTRODUCTION

A spiral galactic disk is usually regarded as a two-dimensional plane when its thickness is ignored in research about its character, because its diameter is much larger than its thickness. In 1987, Binney & Tremaine calculated the period of a star near the Sun in the upright direction of the galactic plane by using two models. The results are $5\times10^7 - 6\times10^7$ yr for the two-dimensional model and $1.1\times10^8$ yr for the three-dimensional model. The latter one is close to the result from actual observation. The two-dimensional model is not accurate when subjected to more detailed analysis of spiral galaxies including the Milky Way Galaxy (whose radius is 10 kpc and thickness is 0.3 pc); i.e., the thickness of the spiral galaxy cannot be ignored. As a result, people have begun to seek a variety of more realistic three-dimensional models of galactic disks.

The thickness of spiral galactic disks is one of the most basic and important parameters in the associated three-dimensional model, from which the strength of self-gravitation in the radial direction and the $z$-direction, which is vertical to the galactic plane, can be derived. In addition, the mass of the galactic halo can be further estimated, the local stability of the galactic disk and the group velocity of the density wave can be studied. More data on the thickness of spiral galactic disks are very important to further amend the statistically theoretical results about galactic dynamics. It is very meaningful to provide the thickness data for a number of spiral galaxies, because the number of galaxies with known thickness data is still small. With the development of telescopic technology, especially the improvement of CCDs, more legible and exact images can be observed. The thickness of more galaxies can be derived from the analysis of their images.

De Vaucouleurs (1958) made a detailed study of photovoltaic metering on M31, which was used to calculate the thickness of M31. van der Kruit & Searle (1981) developed a method for measuring the thickness of edge-on spiral galaxies by fitting the distribution of their surface brightnesses. Peng (1988) proposed a new method to calculate the thickness of non-edge-on spiral galaxies by using the

* Supported by the National Natural Science Foundation of China.

spiral images, and gave thicknesses of four spiral galactic disks. Ma et al. (1997a,b, 1998a,b,c, 2000) gave equivalent thicknesses (the theoretical result of thickness calculations) of many spiral galactic disks using Peng's method. Afterwards, the thickness effect of the galaxy, the dynamic properties of the disk, the stability of the three-dimensional disk and the velocity of the density wave were further studied by some scholars (Luo et al. 1999, 2000a,b; Li et al. 2000; Long et al. 2000; Peng et al. 2001, 2002, 2004). Hu et al. (2006b) recently reported that the mass-to-light ratios of face-on spiral galaxies can be derived by using their thicknesses. The thickness data for over 100 galaxies have been acquired by processing the spiral galactic images using Peng's improved method. Zhao et al. (2006) presented a new method to determine the thickness of non-edge-on spiral galaxies by using the solution of the Jeans equation along the $z$-direction. In this work, the new thickness data of 42 spiral galactic disks are calculated by dealing with the sixth release of spiral galactic images from the Sloan Digital Sky Survey (SDSS). New mass-to-light ratios will be calculated by the new data of spiral galactic disks in our future work.

## 2 BASIC THEORIES

Observations have indicated that a galactic disk may contain a thin disk and a thick one, each of which has its own thickness. The thin disk is formed by the galactic stars. The thickness of a spiral galaxy in our work can be derived based on investigating the rigorous expression of the star's perturbed gravitational potential (Hu et al. 2006a,c), so it belongs to the thin disk. The formula below is obtained by researching the gravitational potential of the infinite thin disk and the finite thick galactic disk,

$$\eta = \frac{V_\alpha(\alpha, m, \Lambda, r_0)}{V_{\alpha\to\infty}(m, \Lambda)} = \mathrm{Re}\{e^{i\Lambda \ln 2}\frac{\Gamma[(1+m+i\Lambda)/2]}{\Gamma[(1+m-i\Lambda)/2]}\int_0^\infty J_m(x)\frac{e^{-i\Lambda \ln x}}{x[1+x/(\alpha r_0)]}dx\}\sqrt{m^2+\Lambda^2}, \quad (1)$$

$\eta$ is a decreased degree factor given by Zhao et al. (2004), which is the ratio of the perturbed gravitational potential, $V_\alpha(\alpha, m, \Lambda, r_0)$, in the infinite thin disk compared with the potential, $V_{\alpha\to\infty}(m, \Lambda)$, in the finite thick galactic disk at the forbidden region radius $r_0$. In Equation (1), $\alpha$ is the equivalent thickness factor of a three-dimensional spiral galaxy. $m$ is the number of arms in the galaxy, and $m$ is 2 for most galaxies. $\Lambda$ is the winding level of the logarithmic spiral, which can be derived from fitting the arm with the logarithmic spiral. The polar coordinate of the arm is $(r, \phi)$ and its form is very simple in the galactic plane.

$$r = r_0 e^{\frac{m}{\Lambda}(\phi-\phi_0)}, \quad (2)$$

where $(r_0, \phi_0)$ is the innermost polar coordinate and $r_0$ is the forbidden region radius obtained after discounting the effect of the nuclear-disk by using the software GALFIT. Density wave theory indicates that in the forbidden region radius $r_0$, the arms will disappear because the degraded gravitational potential cannot evoke the self-consistency of the density wave. $\Gamma[(1+m\pm i\Lambda)/2]$ is the gamma function and $J_m(x)$ is the Bessemer function. The pitch angle $\mu$ and the inclination $\gamma$ of the arms are the foundational parameters and are expressed respectively below as

$$\mu = \arctan\frac{m}{\Lambda}, \quad (3)$$

$$\gamma = \arccos\sqrt{1.042\left(\frac{b}{a}\right)^2 - 0.042} + 0.052, \quad (4)$$

where the factors $a$ and $b$ represent respectively the long axis and the short axis of the galaxy.

For the infinite thin disk galaxies, in the original density wave theory, the amplitude of the perturbed gravitational potential in the vicinity of the galaxy's center is still quite strong, and the perturbed density and perturbed gravitational potential are self-consistent. The corresponding arm pattern can be extended inwards from outside of the galactic disk to the galaxy's center. However, for the finite thick disk, the circumstances are different.

In fact, we can assemble the finite thick disk by stacking a number of plane parallel layers. In a layer far from the galactic plane, at a certain distance and parallel to the galactic disk, the planes in different locations ($r$ different) have different distances from the galactic center. When the density perturbs it, because the phases of these layers' perturbed gravitational potential in the galactic disk are different, interference effects will work in the inner zone of the galactic disk's center. As a result, the perturbed gravitational potential is obviously weakened. In fact, the specific numerical calculation shows that the value of the size of $\eta$ decreases when $\alpha\ (= 2/H)$ is reduced, in another word: the thicker the disk, the smaller $\eta$ is (Peng et al. 2001).

In a physical sense, if the amplitude of the perturbed gravitational potential once reduces to half the value of its original infinite thin plate (the corresponding location is $r_0$ and $\eta = 0.5$), its corresponding energy (in direct proportion to the square of the amplitude of gravitational potential) is only a quarter of the infinite thin disk's. At this time, the perturbations of the gravitational potential and the density are in no possible way self-consistent. The self-consistent density wave will disappear and no longer exist in the inner zone of the galactic disk's center. Accordingly, it is impossible to show the arm pattern in the inner zone. The inner zone is the (self-consistent) density waves' forbidden region, and $r_0$ is known as the forbidden region radius.

However, the above is just pure theoretical conjecture. Astronomical observations should be based on actual data. So far, for non-edge-on spiral galaxies, we can really only rely on the Galaxy and M31, whose thicknesses can be obtained from other reliable methods. The value $\eta$ can be calculated from these two galaxies' thicknesses (or $\alpha = 2/H$) (Zhao et al. 2004).

## 3 IMAGES PROCESSED

In this work, all original images are from the Sloan Digital Sky Survey. In our work, the effect of the nuclear-disk, especially the effect of the lightness of the central bulge, is deduced with the use of the software IRAF and GALFIT. Moreover, a lot of information, such as the coordinates of the galactic center, the axial ratio and the direction of the long axis, can be obtained. In the remaining arm images, we directly take points on the arm to fit arms via least squares, and derive $r_0$ and $\Lambda$. Finally, the equivalent thickness of the spiral galactic disk is obtained by the use of the software MATHEMATIC.

SDSS collects the image information in five bands ($g$, $u$, $r$, $i$, $z$) for every galaxy. The former work points out that the images from the five bands give the same equivalent thickness after being processed and fitted. In our work, only the g-band images are processed and fitted because they are clearer. The width of a pixel of the image in the SDSS is $0.369''$ and the distance $D$ of those galaxies is calculated according to Hubble's law ($H_0 = 75\,\mathrm{km\ s^{-1}\ Mpc^{-1}}$). We derived a more accurate radius $r_0$ by repeatedly adjusting the galactic gray-scale with the software IRAF. We replace the radian with the angle of the pixel because the angular resolution of the pixel is very small.

Figure 1 shows the original, processed and fitted images of galaxy PGC 20886, respectively.

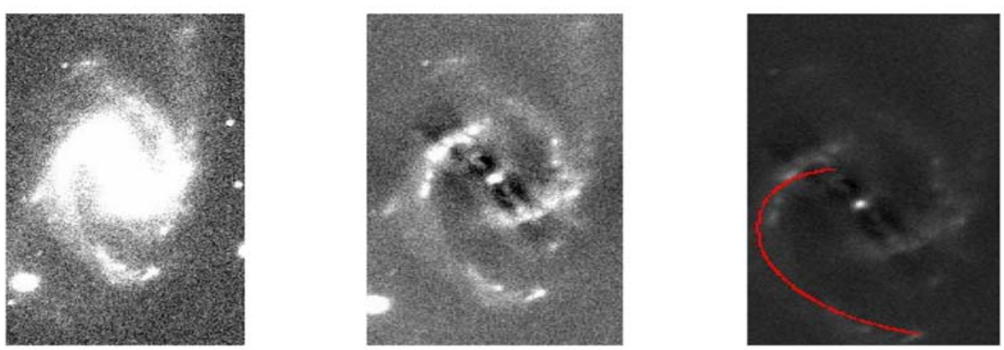

Original image (PGC20886) Processed image (PGC20886) Fitted image (PGC20886)

**Fig. 1** PGC 20886's original, processed and fitted images.

## 4 RESULTS AND ANALYSES

The equivalent thicknesses for 42 spiral galactic disks are given in Table 1, which have the same order of magnitude as other spiral galactic disks given by Ma (1997a,b, 1998a,b,c, 2000) and Hu et al. (2006a,c).

In addition, the error estimates are derived from the formulae of Hu et al.'s articles (2006a,c). From Table 1, one can find that PGC 21443 (radius 420 kpc) has the largest equivalent thickness which reaches 3.631 kpc and that PGC 32614 (radius 2 Mpc) has the smallest equivalent thickness of 0.222 kpc. All the data in Table 1 show that the galactic disk thickness cannot be ignored, especially for more exact studies on galactic disks.

**Table 1** Thicknesses of 42 Spiral Galaxies ($m = 2$)

| PGC | $D$ (Mpc) | $\gamma$ ($^\circ$) | $r_0$ (pixel) | $\mu$ ($^\circ$) | $\Lambda$ | $H$ (kpc) |
|---|---|---|---|---|---|---|
| PGC 00548 | 72.94 | 58.62 | 15.00 | 65.02 | 0.93(±29.77%) | 1.933(±16.93%) |
| PGC 07465 | 93.68 | 65.04 | 7.81 | 83.74 | 0.22(±13.07%) | 1.470(±15.87%) |
| PGC 09582 | 84.68 | 63.15 | 17.00 | 7.79 | 14.64(±20.22%) | 0.369(±34.35%) |
| PGC 09765 | 87.86 | 64.11 | 16.49 | 21.25 | 5.15(±18.80%) | 0.988(±37.20%) |
| PGC 20886 | 95.14 | 68.52 | 9.90 | 88.06 | 0.07(±35.84%) | 1.910(±37.29%) |
| PGC 21443 | 128.50 | 61.14 | 17.12 | 59.18 | 1.19(±25.63%) | 3.631(±23.62%) |
| PGC 21927 | 110.64 | 57.86 | 28.65 | 10.45 | 10.85(±20.50%) | 1.117(±33.59%) |
| PGC 22008 | 128.42 | 50.51 | 10.82 | 55.73 | 1.36(±25.42%) | 2.186(±31.31%) |
| PGC 22734 | 147.06 | 61.14 | 18.44 | 8.91 | 12.76(±22.65%) | 0.796(±25.81%) |
| PGC 22747 | 144.69 | 63.15 | 12.04 | 77.76 | 0.44(±26.61%) | 3.413(±10.42%) |
| PGC 23850 | 56.73 | 49.52 | 25.94 | 34.14 | 2.95(±21.90%) | 1.535(±29.34%) |
| PGC 24499 | 108.56 | 60.08 | 12.44 | 10.96 | 10.33(±17.36%) | 0.497(±36.45%) |
| PGC 25547 | 145.82 | 64.42 | 53.15 | 6.54 | 17.46(±38.09%) | 1.731(±27.82%) |
| PGC 26225 | 197.57 | 64.73 | 7.07 | 44.60 | 2.03(±29.59%) | 1.831(±34.69%) |
| PGC 26357 | 135.35 | 43.42 | 28.84 | 27.79 | 3.80(±22.69%) | 3.388(±11.25%) |
| PGC 27219 | 73.57 | 67.97 | 26.42 | 59.13 | 1.20(±31.95%) | 3.205(±20.54%) |
| PGC 31908 | 199.99 | 65.04 | 8.00 | 5.75 | 19.86(±21.49%) | 0.298(±25.93%) |
| PGC 31917 | 176.18 | 51.94 | 12.08 | 5.80 | 19.69(±34.50%) | 0.396(±14.42%) |
| PGC 32614 | 21.16 | 51.47 | 32.65 | 9.57 | 11.87(±21.47%) | 0.222(±35.08%) |
| PGC 33686 | 241.57 | 56.68 | 18.79 | 13.28 | 8.48(±29.48%) | 1.940(±28.70%) |
| PGC 36148 | 122.30 | 54.19 | 9.85 | 10.10 | 11.24(±15.17%) | 0.394(±31.57%) |
| PGC 36441 | 80.54 | 56.68 | 20.25 | 6.44 | 17.73(±18.57%) | 0.353(±18.08%) |
| PGC 36481 | 90.45 | 60.44 | 17.89 | 52.42 | 1.54(±14.29%) | 2.427(±20.91%) |
| PGC 36574 | 87.67 | 60.44 | 18.87 | 26.57 | 4.00(±38.59%) | 1.376(±33.34%) |
| PGC 37444 | 25.24 | 64.11 | 51.55 | 83.85 | 0.22(±11.76%) | 2.616(±18.56%) |
| PGC 38213 | 74.73 | 57.08 | 28.02 | 18.24 | 6.07(±26.22%) | 1.239(±30.85%) |
| PGC 40816 | 24.90 | 60.08 | 11.18 | 87.25 | 0.10(±34.74%) | 0.564(±23.73%) |
| PGC 41468 | 93.52 | 64.73 | 8.25 | 77.77 | 0.43(±17.37%) | 1.510(±20.64%) |
| PGC 45773 | 113.56 | 41.51 | 17.03 | 50.93 | 1.63(±21.53%) | 2.835(±25.19%) |
| PGC 45921 | 141.04 | 48.50 | 30.36 | 24.50 | 4.39(±13.87%) | 3.319(±28.17%) |
| PGC 46283 | 91.66 | 54.19 | 17.20 | 74.85 | 0.54(±19.47%) | 3.033(±31.19%) |
| PGC 47855 | 94.29 | 52.86 | 12.73 | 87.79 | 0.08(±11.62%) | 2.431(±14.49%) |
| PGC 48333 | 64.44 | 34.08 | 19.10 | 68.11 | 0.80(±18.39%) | 2.243(±33.55%) |
| PGC 48421 | 93.58 | 59.36 | 15.62 | 35.08 | 2.85(±33.49%) | 1.554(±16.86%) |
| PGC 49694 | 112.46 | 50.51 | 10.20 | 73.06 | 0.61(±22.32%) | 2.178(±23.77%) |
| PGC 50719 | 68.46 | 68.25 | 15.52 | 81.55 | 0.30(±20.71%) | 2.120(±25.22%) |
| PGC 52417 | 119.80 | 44.62 | 6.32 | 44.74 | 2.02(±30.70%) | 0.996(±15.26%) |
| PGC 52532 | 109.24 | 49.52 | 16.00 | 5.16 | 22.17(±35.71%) | 0.316(±27.12%) |
| PGC 54039 | 141.58 | 54.19 | 25.81 | 12.76 | 8.83(±17.77%) | 1.537(±20.91%) |
| PGC 56410 | 86.57 | 52.41 | 22.67 | 20.01 | 5.50(±23.47%) | 1.261(±35.98%) |
| PGC 59118 | 148.60 | 57.47 | 15.81 | 50.07 | 1.68(±16.01%) | 3.396(±15.93%) |
| PGC 62037 | 72.80 | 56.68 | 20.30 | 6.41 | 17.82(±39.31%) | 0.317(±35.06%) |

Notes: $D$ is galactic distance, $\gamma$ arms' inclination, $r_0$ forbidden region, $\mu$ pitch angle, $\Lambda$ winding level of the logarithmic spiral, and $H$ is equivalent thickness.

**Acknowledgements** IRAF is a general purpose software system for the reduction and analysis of astronomical data, whose full name is the Image Reduction and Analysis Facility. IRAF is written and supported by the IRAF programming group at the National Optical Astronomy Observatory (NOAO). We are grateful to NOAO for all their efforts. We would like to thank the referee for valuable comments, and thank Y. H. Zhao, W. Sun, Y. Li and M. J. Lan for their good suggestions. This work was supported by the National Natural Science Foundation of China under grant 10778719.

## References

Binney, J., & Tremaine, S. 1987, Galactic Dynamics (Princeton: Princeton University Press)
De Vaucouleurs, G. 1958, ApJ, 127, 487
Hu, T., Peng, Q. H., & Zhao, Y. H. 2006a, A&A, 446, L5
Hu, T., Peng, Q. H., & Zhao, Y. H. 2006b, ChJAA (Chin. J. Astron. Astrophys.), 6, 43
Hu, T., Shao, Z. Y., & Peng, Q. H. 2006c, ChJAA (Chin. J. Astron. Astrophys.), 6, 175
Li, M., Luo, X. L., Peng, Q. H., et al. 2000, Chinese Physics Letters, 17, 466
Long, M., Peng, Q. H., Luo, X. L., et al. 2000, Chinese Physics Letters, 17, 929
Luo, X. L., & Peng, Q. H. 1999, Chinese Physics Letters, 16, 931
Luo, X. L., Peng, Q. H., Long, M., et al. 2000a, Chinese Physics Letters, 17, 932
Luo, X. L., Long, M., Peng, Q. H., et al. 2000b, Acta Astron. Sinica, 41, 424
Ma, J., Peng, Q. H., Chen, R., et al. 1997a, A&AS, 126, 503
Ma, J., Peng, Q. H., & Gu, Q. S. 1997b, ApJ, 490, 51
Ma, J., & Peng, Q. H. 1998a, Science in China A: Mathematics, 41, 557
Ma, J., Peng, Q. H., Li, W. D., et al. 1998b, Acta Astron. Sinica, 39, 28
Ma, J., Peng, Q. H., & Gu, Q. S. 1998c, A&AS, 130, 449
Ma, J., Zhao, J. L., Zhang, F. P., et al. 2000, Acta Astron. Sinica, 41, 172
Peng, Q. H. 1988, A&A, 206, 18
Peng, Q. H., Luo, X. L., et al. 2001, Progress in Astronomy, 19, 397
Peng, Q. H., Peng, F., Chou, C. K., et al. 2002, Ap&SS, 282, 499
Peng, Q. H., Chou, C. K., Lin, Y. H., et al. 2004, New Astronomy, 10, 17
Shang, Z. H., Bao, M. X., Zhang, W. Y., et al. 1992, Acta Astron. Sinica, 33, 371
van der Kruit, P. C., & Searle, L. 1981, A&A, 95, 105
Zhao, Y. H., Peng, Q. H., & Wang, L. 2004, ChJAA (Chin. J. Astron. Astrophys.), 4, 51
Zhao, Y. H., Peng, Q. H., & Hu, T. 2006, A&A, 452, 451